IJCSE International Journal of Computer Sciences and Engineering Open Access
Research Paper Vol.-6, Issue-6, June 2018 E-ISSN: 2347-2693

Multispectral Image Compression with Discrete Wavelet Transformed Improved SPIHT using various Wavelets

Bhagya Raju V[1], K. Jaya Sankar[2], C. D. Naidu[3]

[1] Department of ECE, JNTU Hyderabad, Telangana, India
[2]Department of ECE, Vasavi College of Engineering, Hyderabad, Telangana, India
[3] Department of ECE, VNR VJIET, Hyderabad, Telangana, India

[*]*Corresponding Author: vbhagya01@gmail.com, Tel.: +91-72878-39644*

Available online at: www.ijcseonline.org

Accepted: 03/Jun/2018, Published: 30/Jun/2018

***Abstract*—**The utilization of Multispectral sensors technology has become more and more significant in recent decades due to the extensive usage of capturing Multispectral images used in remote sensing applications. This research work explores a different view of investigating lossy multispectral image compression from a perspective of extracting spectral information. It is an exploitation-based lossy compression which further develops spectral/spatial multispectral image compression to preserve the significant spectral information of objects. In this paper, we present a transformed based DWT with Improved SPIHT algorithm for various existing discrete wavelets. The proposed algorithm, a lossy multispectral image compression method yields better performance results for PSNR, MSE, CR, ENTROPY(H), SSIM and CC with sym8 wavelet when compared with previous well-known compression methods and existing discrete wavelets.

Keywords— Multispectral Images, DWT, ISPIHT, LIBT, LIST.

I . INTRODUCTION TO MULTISPECTRAL IMAGES

The multi-spectral cameras are costly when compared to their RGB counterparts, e.g., a 5 sensor multispectral camera with a resolution of only 1360×1024 cost is very high, when compared to a single-sensor RGB camera with much higher resolution. The high expenditure of multi-spectral cameras is the main setback in widespread applications of such devices in developing countries. The objective of this work is to bring down the amount of such multi-spectral cameras. Most multi-spectral cameras have different sensor arrays for each band of the EM-spectrum. Image acquisition using such separate sensor arrays requires a large number of optical and mechanical parts which contributes to the increased cost and size of the cameras. Many researchers are working on the problem of compressing multispectral images with various encoding schemes. PCA transforms the images in the spectral direction, and its main advantage is that it not only allows the most decorrelation possible among spectral bands, but also the best energy compaction, which in turn results in better mineral classification. On the other hand, the main disadvantage of the PCA is that the covariance matrix, which is used to decorrelate among frequency bands, has to be calculated, and therefore it is data dependent. Many use vector quantization (VQ) and Karhunen-Loeve transform (KLT) on the spectral dimension to explore the correlation between multispectral bands [1].

In this paper, a novel algorithm for lossy compression of Multispectral images based DWT with Modified SPIHT is proposed which provides better picture quality regarding high PSNR than the other compression methods using symlet wavelets. The necessity for image compression of multispectral images is explained in section II. The Proposed Compression Technique for multispectral imageries with Discrete Wavelet Transformed Improved SPIHT by using various wavelets is explained in section III. To further substantiate simulation results, real multispectral image experiments of various datasets like the LAN file of little co river is considered for performance and evaluation analysis. The implementation analysis in terms of CR, MSE, SSIM, PSNR, CC and ENTROPY for different wavelets is compared with DWT SPIHT [2] and DWT ISPIHT [3] algorithms in Section IV. We conclude and present perspectives for future scope of work in Section V.

II. NECESSITY FOR IMAGE COMPRESSION

The Image compression is performed to translate the image information to more compact support to reduce the redundancy of the image data to be able to store or transmit it in a more efficient form [4]. Uncompressed image data is enormous in file size and to store or retrieve/transmit the uncompressed image requires considerable storage capacity and bandwidth. In Multispectral images, there is mainly two

type of redundancy: Spatial Redundancy and Spectral Redundancy. Spatial redundancy refers to the correlation between neighboring pixels which is due to patterning, or self-similarity within an image. Spectral Redundancy occurs due to similarity between different color planes or spectral bands [5].

III. PROPOSED COMPRESSION TECHNIQUE

3.1 Multi - Resolution 2-D wavelet decomposition

In the image processing domain, Wavelet transforms have been proven very advantageous for various applications like image compression, reconstruction, feature extraction, and image registration ([6], [7], [8]). In Discrete Wavelet Transform, a two-dimensional scaling function (x, y), and three two-dimensional wavelet functions, φH(x, y), φV(x, y), and φD(x, y), are required. They measure functional variations, intensities for image along different directions.H measures variations along columns (for example horizontal edges), V measure variations along rows (likes vertical edges) and D corresponds to variations along diagonals. Scaling function measures the smooth regions, and Wavelet functions measure the sharp details of an image using analysis and synthesis filter banks. Each is the product of two one-dimensional functions given by

$$\phi(x,y) = \varphi(x)\varphi(y) \quad (1)$$
$$H(x,y) = (x)\varphi(y) \quad (2)$$
$$V(x,y) = \varphi(x)(y) \quad (3)$$
$$D(x,y) = (x)(y) \quad (4)$$

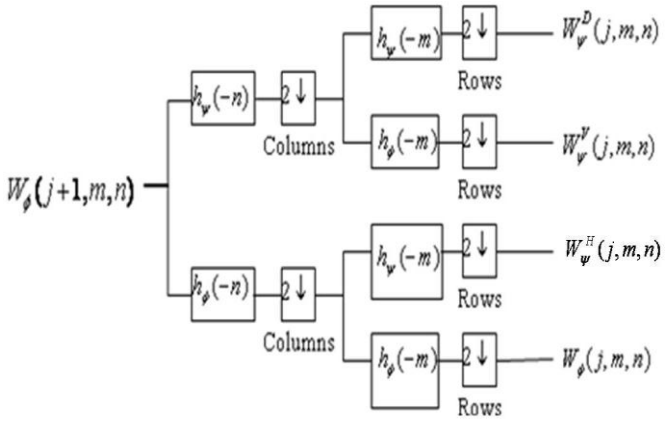

Fig.1: DWT Analysis Filter Bank

The analysis and synthesis filter banks are shown in Fig.1and Fig.2 respectively. The image is sampled, filtered and the individual bands are summed up to give the image from the discrete wavelet components. The decomposition and reconstruction filters are used at analysis and synthesis filter banks respectively. The decomposition filters are similar to decimators and the reconstructions filters are similar to interpolators.

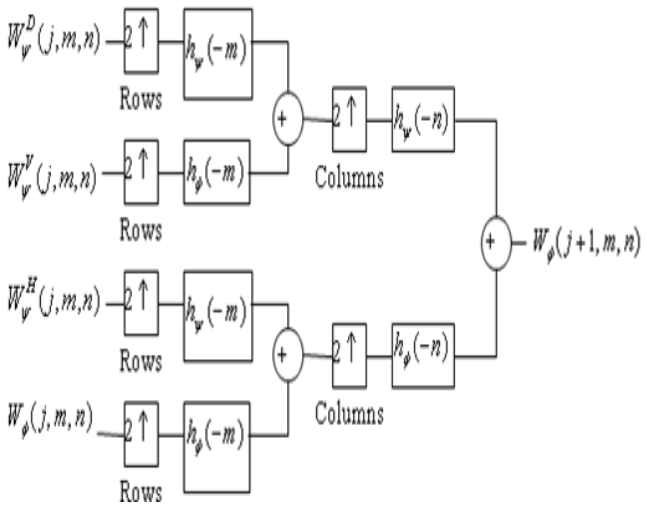

Fig.2: DWT Synthesis Filter Bank

3.2. Wavelet Transformation

Transformation of information of signals into different representations are performed by various mathematical transforms [9].For example Fourier Transforms are used to convert signals from frequency to time domain, but the related information to particular frequencies at specific times is not provided. This drawback is outperformed by means of window based STFT technique where in the information of time along with frequency is obtained for different parts of the signal at different instants of time. However according to Heisenberg's uncertainty principle the resolution gets worse in frequency domain as the resolution of the signal is improved in time domain by zooming the signal on different sections. Hence multiresolution is required to enhance certain parts of the signal in time and remaining parts in frequency domain. The image is represented as a sum of wavelet functions with different scales and locations by means of Wavelet Transform which exhibits high energy compaction and decorrelation properties.

3.2.1 Discrete Wavelet Families

Different families of wavelet are designed and developed for DWT which are compactly supported by means of low pass and high pass analysis and synthesis filters for orthogonality and biorthogonality. Haar, Daubechies, Symlets, Coieflets, Meyer, Biorthogonal and Morlet etc are few families of wavelets available [10]. The daubechies, haar, symlets, Meyer, biorthogonal, reverse biorthogonal and coiflets are supported by orthogonal wavelets. Wavelets are chosen for any particular application based on the ability to analyze the signal and its scaling function [11].

3.2.2 Haar Wavelet

The simplest possible wavelet was proposed by Alfred Haar in 1909 named Haar wavelet which is a very fast transform whose basis vectors are sequentially ordered. Haar wavelets is a sequence of rescaled "square shaped" functions in mathematics whose main disadvantage is it is not continuous which cannot be differentiated and resembles a step function. It represents same wavelets as Daubechies 1.Haar transform has poor energy compaction for images and it is real and orthogonal i.e. Hr=*Hr and the basis vectors of Haar matrix are always sequentially ordered [12].

3.2.3 Daubechies wavelets

The search for scaling function which are compactly supported, orthogonal and continuous was the major problem in the development of wavelets during 1980's was overcome by Ingrid Daubechies by inventing compactly supported orthonormal wavelets thus making discrete wavelets analysis practicable[13]. Daubechies wavelet transform are similar to Haar wavelets which are defined by computing running averages and differences through scalar products with scaling signals and wavelets. Higher order Daubechies wavelets are defined by DBN where N denotes the order of wavelet and the number of vanishing moments for given support width N=2A where A is highest number of vanishing moments.

3.2.4 Symlet wavelets

Since Daubechies wavelets select the minimum phase square root where energy concentrates near the starting point of their support are not symmetric. Whereas symlets are nearly symmetric wavelets proposed by Daubechies as modifications to the Db family which select each other set of roots for close symmetry with linear complex phase. Remaining other properties of Daubechies and symlets families are similar apart from symmetry [14, 15].The peak signal to noise ratio (PSNR) of the reconstructed and decompressed image is improved using symlets which are shown below.

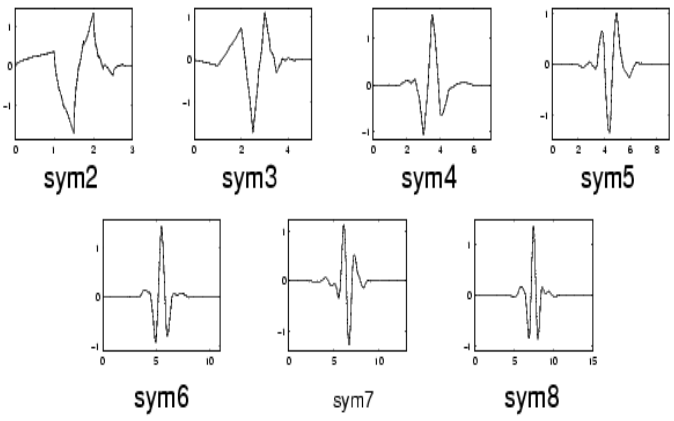

Fig.3: Symlet Wavelets

3.2.5 Coiflet wavelets

Daubechies wavelets and coiflets are similar to a certain extent but the vanishing moments are computed not only for wavelet function but also for scaling function in coiflet wavelet transform. Some useful features of this wavelet are i) Good approximation of polynomial functions at different resolutions is obtained by this method which increases the computational efficiency of the analysis. ii) Frequency and time information in an integral obtained with this wavelet where visualization of signal characteristics can be easily achieved.

3.2.6 Biorthogonal & Reverse Biorthogonal wavelets

These families of wavelets have applications in image and signal processing which are realized by Matrix-vector products with sparse, structured matrices. The dual scaling and wavelet functions with following properties are used. They are zero outside a segment and calculations are simple. Filters associated are symmetric in nature. The asymmetric nature causes artifacts at borders which are overcome by Meyer wavelets to some extent. The reverse biorthogonal wavelets are symmetric, not orthogonal and biorthogonal.

3.2.7 Meyer wavelets

The Meyer wavelet is an orthogonal wavelet proposed by Yves Meyer. It is infinitely differentiable with infinite support and defined in frequency domain in terms of function ν. There are many different ways for defining this auxiliary function, which yields variants of the Meyer wavelet.

3.3. Improved Set Partitioning of Hierarchical Trees

The ISPIHT algorithm is a more efficient implementation of EZW (Embedded Zero Wavelet) [16] [17] algorithm which was presented by Shapiro. After applying wavelet transform to an image, the ISPIHT algorithm partitions the decomposed wavelet into significant and insignificant partitions based on the following function:

$$Sig_n(T) = \begin{cases} 1, max_{(i,j)\epsilon T}|c_{i,j}| \geq 2^n \\ 0, other\ wise \end{cases} \quad (5)$$

Here $Sig_n(T)$ is the significance of a set of coordinates T, and $c_{i,j}$ is the coefficient value at coordinate (i, j). The maximum number of bits required to represent the largest coefficient in the spatial orientation tree is obtained and represented by

$$n_{max} = [log_2(max_{(i,j)}|c_{i,j}|)] \quad (6)$$

There are two passes in the algorithm- the sorting pass and the refinement pass. The ISPIHT encoding process utilizes three lists *LIBT* (List of Insignificant Block Test) – It contains individual coefficients as a block that have magnitudes smaller than the thresholds *LIST* (List of Insignificant Sets Test) – It contains set of wavelet coefficients that are defined by tree structures and are found to have magnitudes smaller than the threshold. *LSP* (List of Significant Pixels) – It is a list of pixels found to have

magnitudes larger than the threshold (significant) and *VT* (vector Tree) corresponding to *LIST*. The sorting pass is performed on the above three lists. It comprises of two passes subordinate and refinement passes. The coefficients which are yet to be significant are there in subordinate pass and the coefficients which are already found to be significant are refined in their magnitude by sending the nth most significant bit of LSP.

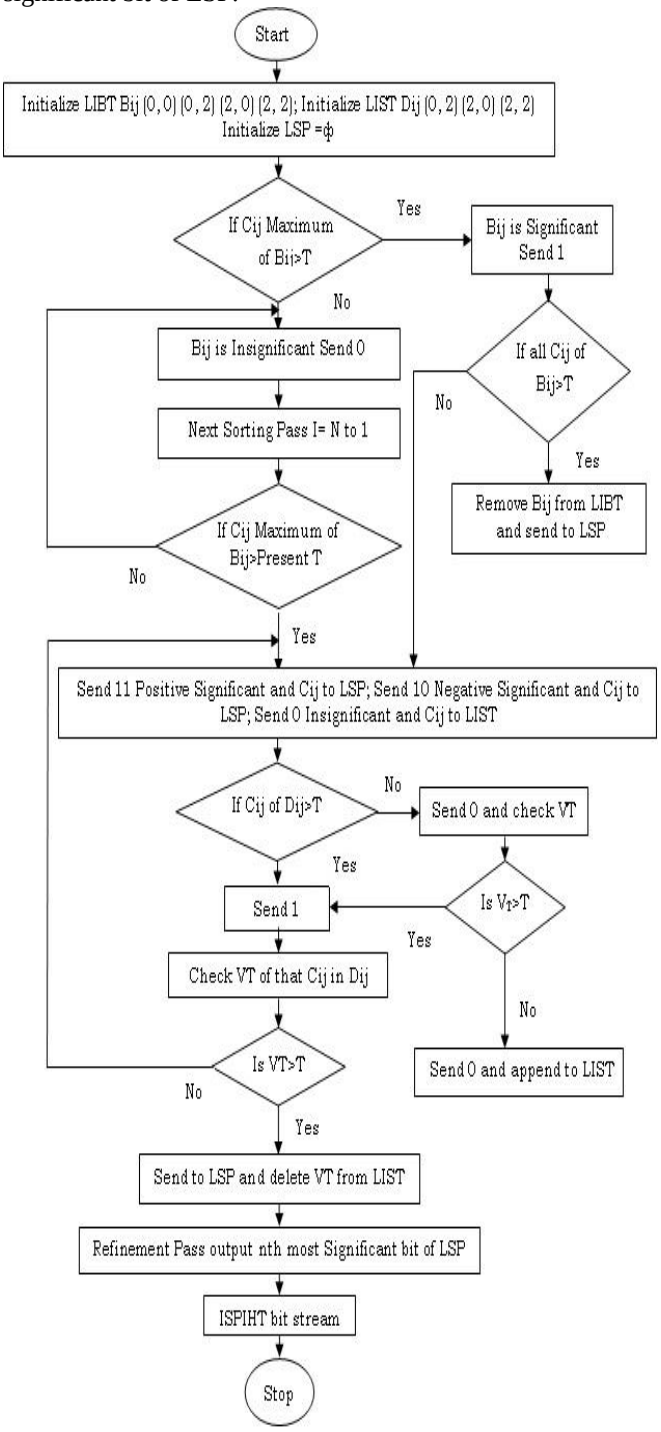

Fig.4: Design Flow of DWT ISPIHT algorithm

IV. PERFORMANCE EVALUATION

In this proposed work discrete wavelet transform along with various wavelets are applied on image matrix to obtain the wavelet coefficients which are then quantized and encoded using Improved SPIHT coder. Real multispectral image experiments of various datasets which contains a 7-band 512-by-512 Land sat image and a 128-byte header followed by the pixel values, which are band interleaved by line (BIL) in order of increasing band number. They are stored as unsigned 8-bit integers, in little-endian byte order and the Real bands 4, 3, 2 from the LAN file are captured using the MATLAB(R) function multiband read. The proposed method with DWT ISPIHT exploits symmetric nature of symlet8 wavelet and effectively compresses the image data with good resolution when compared to the conventional methods like DCT KLT, DWT SPIHT in terms of PSNR, MSE, CR, ENTROPY, SSIM and CC. The algorithm is implemented in mat lab R2016b shown in Fig.5.The comparative results for DWT SPIHT and DWT ISPIHT in terms of various existing wavelets are shown in Table I and Table II respectively. Their graphs are represented in Fig.6 and Fig.7 respectively.

4.1. Mean Square Error

In the MSE measurement the total squared difference between the original signal and the reconstructed one is averaged over the entire signal. Mathematically,

$$MSE = \frac{1}{N}\sum_{i=0}^{N-1}\left(\hat{x}_i - x_i\right)^2 \quad (7)$$

Where is $\hat{x}_i$ the reconstructed value of x_i , N is the number of pixels. The mean square error is widely used because of its convenience.

4.2. Peak Signal to Noise Ratio

A measurement of MSE in decibels on a logarithmic scale is the Peak Signal-to-Noise Ratio (PSNR), which is a popular standard objective measure of the lossy codec.

$$PSNR = 10 \log_{10} [255^2 / MSE] \quad (8)$$

4.3. Entropy

The entropy is the measure of an amount of information of the pixels contained in an image given by

$$H = -\sum_{k=0}^{M-1} p_k \log_2(p_k) \quad (9)$$

Where *M* represents the number of gray levels and p_k the probability associated with gray level *k*.

4.4. Correlation Coefficient

The correlation coefficient (CC) is given by

$$r = \frac{\sum_i (x_i - x_m)(y_i - y_m)}{\sqrt{\sum_i (x_i - x_m)^2}\sqrt{\sum_i (y_i - y_m)^2}} \quad (10)$$

DWT	PSNR	MSE	CR	H	SSIM	CC
Bior1.3	28.858	84.612	1.4971	6.1836	0.98562	0.91891
Bior2.4	29.247	77.321	1.4579	6.2710	0.98679	0.92467
Bior5.5	29.621	70.954	1.4785	6.2866	0.98756	0.93115
Coif1	29.767	68.608	1.5048	6.2576	0.98745	0.93333
Coif5	30.318	60.421	1.5043	6.2826	0.98923	0.94160
Db3	29.982	65.290	1.5414	6.2829	0.98901	0.93654
Db5	29.019	81.487	1.5159	6.2879	0.98825	0.92076
Db10	30.155	62.738	1.5112	6.2925	0.98971	0.93908
Dmey	30.392	59.403	1.5136	6.2859	0.98988	0.94244
Haar	29.115	79.705	1.3864	5.9362	0.98826	0.92168
Rbio1.3	30.062	64.091	1.3803	6.2483	0.98975	0.93766
Rbio5.5	29.182	78.492	1.5498	6.2871	0.98542	0.92351
Rbio6.8	30.039	64.438	1.5293	6.2846	0.98888	0.93770
sym6	30.219	61.818	1.5293	6.2779	0.98915	0.94014
sym8	**30.294**	**60.761**	**1.5181**	**6.2776**	**0.98938**	**0.94109**

where, xi and yi are intensity values of ith pixel in 1st and 2nd image respectively. Also, xm and ym are mean intensity values of first and second image respectively. The correlation coefficient has the value of r =1 if the two images are absolutely identical, r= 0 if they are completely uncorrelated and r= -1 if they are anti-correlated.

4.5. Compression Ratio

Compression Ratio is determined as the ratio of the original dataset to the compressed dataset. It gives the measurement of the data compressed without really affecting the overall size of the image. The number of bits used to represent a single pixel gets reduced thereby compressing the image without loss of generality.

CR=original image/compressed image (11)

4.6. Structural Similarity Index Matrix

The motivation behind the structural similarity approach is to measure the image quality concerning a human visual system (HVS) which has not designed for detecting imperfections or errors. Given any two images (of image patches) x and y which is to be compared, *luminance* are estimated as the mean of each image.

$$\mu_x = \frac{1}{N}\sum_{n=1}^{N} x_n \quad (12)$$

Contrast is estimated using standard deviation as

$$\sigma_x = \sqrt{\frac{1}{N-1}\sum_{n=1}^{N}(x_n - \mu_x)^2} \quad (13)$$

,and *structure* are estimated from the image vector x by removing the mean and normalizing by the standard deviation.

$$SSIM(x,y) = \left(\frac{2\mu_x\mu_y + C_1}{\mu_x^2 + \mu_y^2 + C_1}\right)\left(\frac{2\sigma_x\sigma_y + C_2}{\sigma_x^2 + \sigma_y^2 + C_2}\right)\left(\frac{\sigma_{xy} + C_3}{\sigma_x\sigma_y + C_3}\right) \quad (14)$$

Table I: Comparative Results of various wavelets for DWT SPIHT for 0.4 bpp of a little co river multispectral Image.

Table II: Comparative Results of various wavelets for DWT ISPIHT for 0.4 bpp of a little co river multispectral Image

DWT	PSNR	MSE	CR	H	SSIM	CC
Bior1.3	39.317	7.6084	2.9394	6.2896	0.98065	0.99264
Bior2.4	40.015	6.479	2.9956	6.2850	0.98093	0.99411
Bior5.5	39.935	6.8005	2.9956	6.2882	0.98242	0.99381
Coif1	39.949	6.5788	2.9614	6.2907	0.98137	0.99385
Coif5	40.111	6.3374	2.9663	6.2928	0.98292	0.99412
Db3	40.009	6.5012	2.9882	6.2954	0.98354	0.99387
Db5	39.977	6.5366	2.9907	6.2885	0.98224	0.99397
Db10	39.969	6.5483	3.0029	6.2985	0.97808	0.99387
Dmey	40.202	6.2067	2.9785	6.2948	0.98163	0.99407
Haar	39.787	6.8281	2.9467	6.2694	0.98032	0.99325
Rbio1.3	40.276	6.1018	2.9638	6.2915	0.98093	0.99434
Rbio5.5	39.704	6.9606	2.9882	6.2921	0.97992	0.99345
Rbio6.8	39.897	6.6579	2.9956	6.3002	0.98008	0.99378
sym6	40.291	6.0800	3.0053	6.2922	0.97912	0.99437
sym8	**40.308**	**6.0571**	**3.0151**	**6.2876**	**0.98125**	**0.99428**

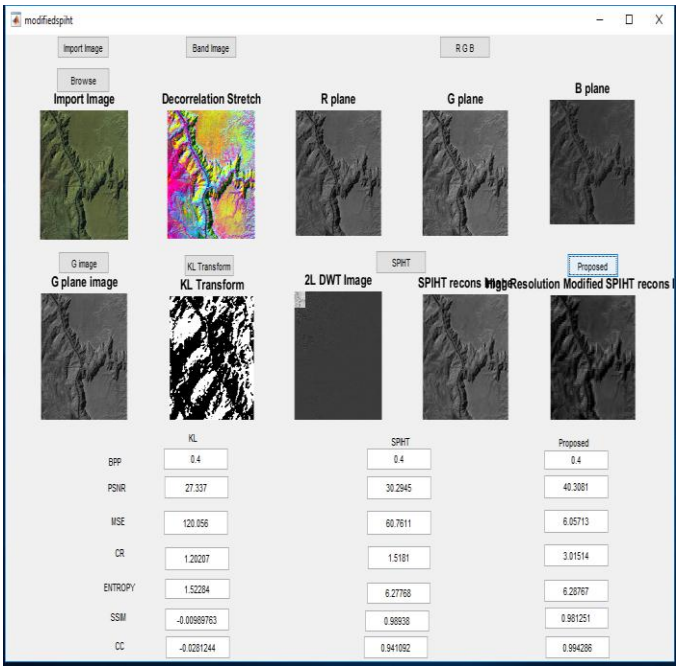

Fig.5: MATLAB Results for sym8 wavelet transform for 0.4 bits per pixel of little co river multispectral image

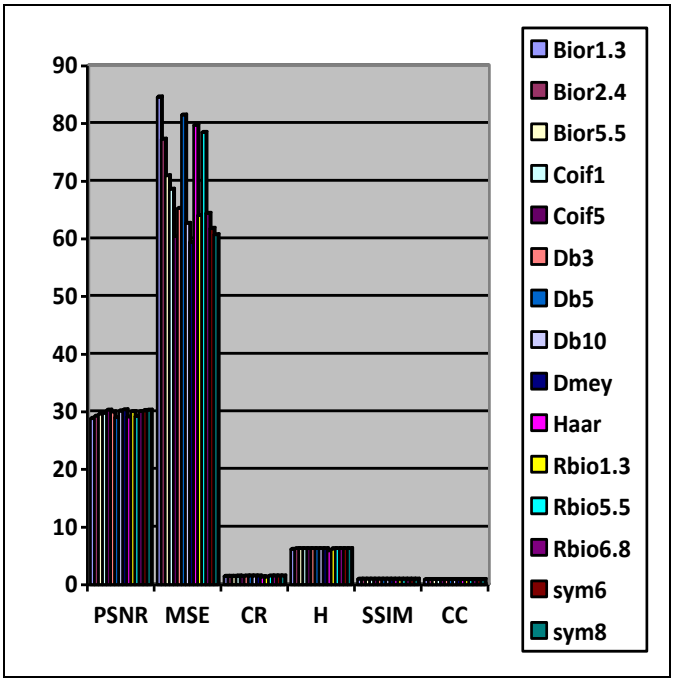

Fig.6: Comparative Results of various wavelets for DWT SPIHT shown graphically for 0.4 bpp of little co river multispectral Image

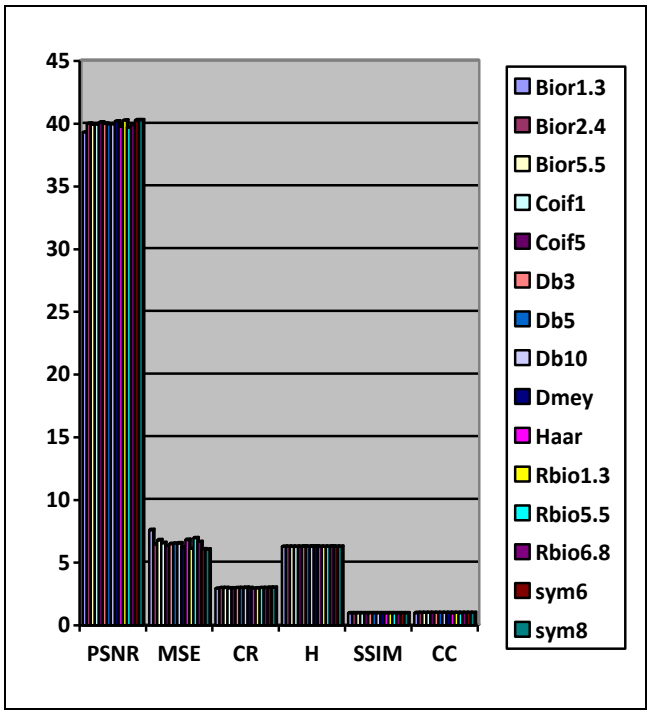

Fig.7: Comparative Results of various wavelets for DWT ISPIHT shown graphically for 0.4 bpp of little co river multispectral Image

V. CONCLUSION

In this proposed work an existing discrete wavelet transform symlet8 with more symmetry and Improved SPIHT algorithm is used for optimal bit-allocation of multispectral images. The spectral correlation which exists in the biorthogonal subclasses is exploited and the quantized DWT wavelet coefficients are encoded by ISPIHT encoder. We compared the results obtained with our technique with DWT SPIHT technique and got superior results. This work has shown that the compression of an image can be improved by considering spectral and temporal correlations in addition to spatial redundancy. The future work aims at extending this frame work for colour images, video compressions, and de-noising applications.

REFERENCES

[1] Xiaoli Tang and William A. Pearlman, "Hyperspectral Data Compression Three-Dimensional Wavelet-Based Compression," Chapter in *Hyperspectral Images*,Kluwer Academic Publishers 2005.

[2] Francesco Rizzo, Bruno Carpentieri, Giovanni Amott and Jame A. Storer, "Low-Complexity Lossless Compression of Hyperspectral Imagery via Linear Prediction," *IEEE Signal Processing Letters*, vol.12,February 2005.

[3] Ian B and Joan S S 2010 IEEE Trans. Geosci. Remote Sens. 487 2854.

[4] M. Ben-Ezra, Z. C. Lin, and B. Wilburn. Penrose pixels: Superresolution in the detector layout domain. In *ICCV*,2007.

[5] H. Chang, D. Y. Yeung, and Y. Xiong. Super-resolution through neighbour embedding. In *CVPR*, volume 1, pages 275–282,2004.

[6] Jian Sun, Jian Sun and Heung-Yeung "Gradient Profile Prior and Its Applications in Image Super-Resolution and Enhancement," IEEE TIP, Vol. 20, pp 1529-1542,2011.
[7] S.G. Mallat, "A Theory for Multiresolution Signal Decomposition: The Wavelet Representation, " *IEEE Transactions on Pattern Analysis and Machine Intelligence*, vol. 11, No. 7, July1989.
[8] C.K. Chui, An Introduction to Wavelets, *Wavelet Analysis and its Applications*, Volume 1, Academic Press,1992.
[9]. Kareen Lees,"Image Compression using Wavelets" in may 2002.
[10] Sonal and Dinesh Kumar,"A study of various Image compression techniques", Guru Jhmbheswar university of science and technology, Hisar
[11] Marta Mrak and Sonia Grig,"Picture quality Measures in image compression systems", EUROCON 2003 Ljubljana, Slovenia.
[12] Michail Shnaider, Andrew P Paplinski,"Wavelet transform in image coding".
[13] Priyanka singh, Priti singh," JPEG image Compression based on Biorthogonal, coiflets and Daubechies Wavelets"..
[14] Faisal Zubir Quereshi, "Image Compression using Wavelet Transform".
[15] Mahesh S.Chavan, Nikos Mastorakis, Manjusha N.Chavan,"Implementation of SYMLET Wavelets to Removal of Gaussian Additive Noise from Speech Signal".
[16] K.Sayood, "Introduction to Data Compression", 2nd edition, Academic Press, Morgan Kaufman Publishers,2000.
[17] "Multispectral Image Compression for various band images with high Resolution Improved DWT SPIHT". SERSC: Science & Engineering Research Support Society International Journal of signal processing, image processing and pattern recognition ISSN: 2005-4254 Volume 9, No.2 (2016) pp.271-286

